HHS Public Access

Author manuscript

Biochemistry. Author manuscript; available in PMC 2019 April 23.

Published in final edited form as:

Biochemistry. 2016 October 25; 55(42): 5917–5926. doi:10.1021/acs.biochem.6b00826.

Thermodynamics of nanobody binding to lactose permease

Parameswaran Hariharan[a], **Magnus Andersson**[b], **Xiaoxu Jiang**[c], **Els Pardon**[d,e], **Jan Steyaert**[d,e], **H. Ronald Kaback**[c,f,g,§], and **Lan Guan**[a,§]

[a]Department of Cell Physiology and Molecular Biophysics, Center for Membrane Protein Research, School of Medicine, Texas Tech University Health Sciences Center, Lubbock, TX 79430, USA

[b]Department of Theoretical Physics and Swedish e-Science Research Center, Science for Life Laboratory, KTH Royal Institute of Technology, SE-171 21 Solna, Sweden

[c]Department of Physiology, University of California, Los Angeles, CA 90095, USA

[d]VIB Center for Structural Biology Research, VIB, 1050 Brussel, Belgium

[e]Structural Biology Brussels, Vrije Universiteit Brussel, Pleinlaan 2, Brussel, 1050, Belgium

[f]Department of Microbiology, Immunology and Molecular Genetics, University of California, Los Angeles, CA 90095, USA

[g]Molecular Biology Institute, University of California, Los Angeles, CA 90095, USA

Abstract

Camelid nanobodies (Nbs) raised against the outward-facing conformer of a double-Trp mutant of the lactose permease of *Escherichia coli* (LacY) stabilize the permease in outward-facing conformations. Isothermal titration calorimetry is applied herein to dissect the binding thermodynamics of two Nbs, one that markedly increases access to the sugar-binding site and another that dramatically increases affinity for galactoside. The findings presented here show that both enthalpy and entropy contribute favorably to binding of the Nbs to WT LacY and that Nb binding to double-Trp mutant G46W/G262W is driven by greater enthalpy at an entropic penalty. Thermodynamic analyses support the interpretation that WT LacY is stabilized in outward-facing conformations similar to the double-Trp mutant with closure of the water-filled cytoplasmic cavity through conformational selection. The LacY conformational transition required for ligand binding is reflected by a favorable entropy increase. Molecular dynamics simulations further suggest that the entropy increase likely stems from release of immobilized water molecules primarily from the cytoplasmic cavity upon closure.

Graphical Abstract

[§]Corresponding authors: Lan Guan, Lan.Guan@ttuhsc.edu; H. Ronald Kaback, rkaback@mednet.ucla.edu.

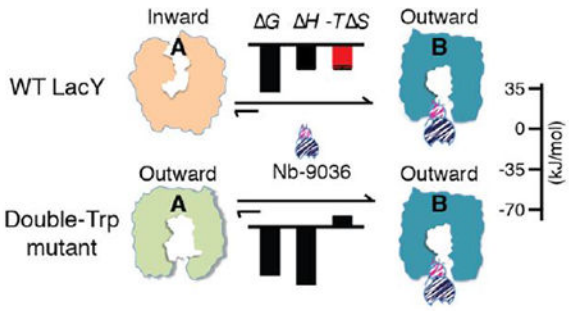

Keywords

isothermal titration calorimetry; protein-protein interactions; sugar binding; conformational transition; entropy/enthalpy; symporters

The lactose permease of *Escherichia coli* (LacY) catalyzes galactoside/H^+ symport[1, 2], and crystal structures demonstrate that the N- and C-terminal six-helix bundles surround a central aqueous cavity[3–8]. Most X-ray structures exhibit an inward (cytoplasmic)-facing conformation with a large water-filled cavity[3–6] (Fig. 2a). Multiple independent lines of evidence[9–12] indicate that the inward-facing conformation represents the lowest free-energy state of LacY in the absence of bound galactoside in either the membrane-embedded or detergent-solubilized states. A double-Trp mutant (G46W/G262W LacY) shifts the lowest energy state of LacY into an outward (periplasmic)-facing conformation[13] that crystallizes with an occluded galactoside. While this conformation has a narrow opening to the periplasm, it is tightly sealed to the cytoplasm(Fig. 2b)[7, 8]. In the outward-facing mutant structure, the galactopyranoside moiety is completely liganded by side chains from both the N- and C-terminal bundles[7, 8]. Galactoside binding induces a relatively large conformational change that allows LacY to expose sugar- and H^+-binding sites to either side of the membrane via an alternating-access mechanism (reviewed in[9, 14]). Evidence has also been presented indicating that sugar binding involves an induced-fit mechanism, which drives LacY into an occluded intermediate state[7].

In order to stabilize WT LacY in an outward-facing conformation for crystallization and structure determination, camelid single-domain nanobodies (Nbs) were raised against a double-Trp mutant[15]. Nine Nbs completely inhibit active lactose transport by right-side-out membrane vesicles containing WT LacY, three inhibit partially, and one does not inhibit significantly[15]. The inhibitory Nbs bind to the periplasmic side of LacY with low nanomolar affinity and stabilize LacY in outward-facing conformations[15, 16]. Based on stopped-flow fluorimetric measurements[15], Nb-9036 increases periplasmic access of the WT to *p*-nitrophenyl-α-D-galactopyranoside (α-NPG) and also increases affinity for α-NPG by ~500-fold for the WT and ~80-fold for the mutant by decreasing the dissociation rate. In contrast, Nb-9065 exhibits little effect on the sugar-binding kinetics with the mutant, but dramatically increases periplasmic access of α-NPG to the sugar-binding site of the WT to a level similar to the outward-facing mutant. Thus, Nb-9065 likely stabilizes the WT in a conformation similar to that of the mutant, and either Nb stabilizes the WT LacY in outward-facing conformations similar to that of the Nb-bound mutant[15].

Recently, isothermal titration calorimetry (ITC) was utilized to study the thermodynamics of ligand binding in membrane transport proteins[17–21]. Binding thermodynamics of the cytosolic phosphotransferase protein IIA^{Glc} to the cytoplasmic face of LacY[18] or melibiose permease (MelB)[19], a galactoside/Na^+ symporter[22–24], have been determined. Although similar binding affinities are observed for the two permeases, thermodynamic features of the binding differ. With *Salmonella typhimurium* melibiose permease ($MelB_{St}$), which crystallizes in an outward-facing conformation[25], IIA^{Glc} binding is exothermic and driven by enthalpy with entropic compensation[19]. In contrast, with LacY, which favors an inward-facing conformation, binding is endothermic and driven primarily by entropy at the cost of enthalpy[18]. Entropy-driven binding has often been interpreted as a hydrophobic effect caused by release of low-entropy immobilized water molecules from hydrophobic interactions between a ligand and the binding surface[26–28]. However, it has been suggested that large global conformational transitions in LacY and favorable solvation entropy make the primary contribution to the increase in entropy favored by IIA^{Glc} binding[18]. In order to examine further the correlation between entropy and conformational changes, the thermodynamics of Nb-9036 or Nb-9065 binding to LacY or the double-Trp mutant, as well as the interplay with sugar and/or IIA^{Glc}, are determined here. The data support the conclusion that conformational selection is involved in Nb binding to WT LacY, which is promoted by galactoside binding. Furthermore, the conformational transition of WT LacY required for ligand binding--whether the ligand is Nb, a galactoside or IIA^{Glc}--is reflected by a favorable entropy increase. Molecular dynamics (MD) simulations suggest that the inward-facing state contains a considerably higher population of immobilized water molecules and displays greater conformational flexibility compared to those in the outward-facing state. Therefore, the entropy increase observed upon Nb binding to WT LacY is likely due to release of bound water molecules mainly from the cytoplasmic cavity upon closure rather than an increase in protein conformational dynamics.

Experimental Procedures

Reagents.

Nitrophenyl-α-galactoside (α-NPG) and nitrophenyl-α-glucoside were purchased from Sigma-Aldrich, and undecyl-β-D-maltopyranoside (UDM) was from Anatrace.

Plasmids and strains.

Construction of plasmids pT7-5/LacY[3] and pT7-5/G46W/G262W LacY[7], each with a His-tag at the C-terminus to allow metal-affinity purification, has been described. The T7-based expression plasmid p7XNH3/IIA^{Glc}-NH10 encoding *E. coli* IIA^{Glc} with a 10-His tag and a 9-residue linker at the N-terminus were constructed as described[19]. Overexpression of IIA^{Glc} or LacY was performed in the *E. coli* T7 Express strain (NEB) or XL1 Blue, respectively.

Nb expression and purification.

Nb-9036 and Nb-9065 were expressed and purified as described[29]. Briefly, the cells were grown in LB broth with 2% glucose, 1 mM $MgCl_2$, and 100 mg/L ampicillin at 37 °C. Overnight cultures were inoculated (1:100, vol/vol) into Terrific Broth containing 0.1% glucose, 2 mM $MgCl_2$, and 100 mg/L ampicillin and shaken at 37 °C; 1 mM IPTG was

added when A_{600} = 0.7, and cells were then shaken at 28 °C overnight. Cells were harvested by centrifugation, and the secreted Nb-9036 or Nb-9065 in the periplasm was obtained by osmotic shock, and purified using cobalt-NTA affinity chromatography. Buffer exchange was carried out to match the LacY solution by dialysis.

IIA^{Glc} expression and purification.

Expression and purification of IIA^{Glc} were carried out as described[19]. IIA^{Glc} in 20 mM Tris-HCl (pH 7.5), 100 mM NaCl, and 10% glycerol was purified by cobalt-affinity chromatography and concentrated to approximately 100 mg/ml. Purified IIA^{Glc} is unphosphorylated [19]. UDM was added to match the LacY solution prior to ITC measurements.

LacY expression and purification.

Cell growth and protein purification of LacY were carried out as described[3, 18]. The purified protein was dialyzed with 20 mM Tris-HCl (pH 7.5), 100 mM NaCl, 0.035% UDM, and 10% glycerol at 20 mg/mL, flash-frozen in liquid nitrogen, and stored at −80 °C.

Protein assay.

The Micro BCA Protein Assay (Pierce Biotechnology, Inc.) was used for the protein concentration measurement.

BN-PAGE.

Blue native-12% PAGE[30] was run at 150 V for 3 h at 4 °C. All samples were supplemented with 0.12% UDM.

ITC.

ITC measurements were performed in a Nano Isothermal Titration Calorimeter (TA Instruments). LacY in complex with Nb or IIA^{Glc} was placed in the sample cell with a reaction volume of 163 μL. The titrant (Nb, IIA^{Glc}, or α-NPG) was prepared in a buffer similar to the titrand in the sample cell, and 2-μL aliquots were injected incrementally into the sample cell at an interval of 300 sec with constant stirring at 250 rpm. For sugar binding to LacY or the LacY:Nb complex, α-NPG were dissolved in dimethyl sulfoxide (DMSO), and diluted with assay buffer to 1 mM containing 0.5 % DMSO. DMSO was added to the protein samples so that the buffers matched. Titration of nitrophenyl-α-glucoside under identical conditions was used as a control.

ITC data process was performed as described[18]. A correction for the heat of dilution was applied for a baseline-corrected thermogram by subtracting the integrated peak area from a constant estimated from the convergence value of the final injections. The corrected heat change (ΔQ) was plotted against the molar ratio of titrant verses titrand. Binding stoichiometry (N), the association constant (K_a), and enthalpy change (ΔH) were directly determined by fitting the data using the one-site independent binding model provided by the NanoAnalyze version 2.3.6 software. $K_d = 1/K_a$; $\Delta G = -RT \ln K_a$; R, gas constant, 8.315 J/K mol; T, absolute temperature. ΔS values were obtained by calculation using the equation $T\Delta S = \Delta H - \Delta G$.

Statistics.

Unpaired *t*-test is used for data analyze. $P > 0.1$, the differenc is considered to be not statistically significant (ns); $0.1 < P > 0.05$, not quite statistically significant ($^{\pm}$); $0.05 < P > 0.01$, statistically significant (*); $0.01 < P > 0.001$, very statistically significant (**).

Building the model systems.

A simulation of the inward-facing crystal structure of LacY (PDB ID, 2V8N) inserted into POPE lipids published[31], was extended from 85 ns to 210 ns. The outward-facing crystal structure (PDB ID: 4ZYR) from the double-Trp mutant LacY was mutated back to wild type, and the missing loop (residues 191-206) was build using the software Modeller[32]. The ligand α-NPG parameters were determined using MATCH[33] as described[34]. The protein model was inserted by aligning the protein center-of-mass to a POPE lipid bilayer containing 490 lipids generated by the CHARMM-GUI membrane builder[35]. The system was subsequently solvated by 18,433 water molecules, and 59 Na^+ and 67 Cl^- ions were added to achieve electric neutrality and a 150 mM salt concentration. The simulation system was relaxed using a 10,000-step conjugate-gradient energy minimization followed by gradual heating, from 0 to 310 K over 120 ps. The lipids followed by the water molecules were then allowed to adjust to the restrained protein structure during consecutive 5 ns equilibration steps.

Simulation.

The MD simulation was run with the NAMD 2.9 software package [36]. The CHARMM22 including CMAP correction and CHARMM36 force fields[37, 38] were used for protein and lipids, respectively, and the TIP3P model was used for the water molecules[39]. A time step of 1 fs was used to integrate the equations of motion, and a reversible multiple time step algorithm[40] of 4 fs was used for the electrostatic forces and 2 fs for short-range, non-bonded forces. The smooth particle mesh Ewald method[41, 42] was used to calculate electrostatic interactions. The short-range interactions were cut off at 12 Å. All bond lengths involving hydrogen atoms were held fixed using the SHAKE[43] and SETTLE[44] algorithms. A Langevin dynamics scheme was used for thermostating and Nosé-Hoover-Langevin pistons were used for pressure control[45, 46]. Molecular graphics and simulation analyses were generated with the VMD 1.9.1 software package[47].

Results

Nb binding to double-Trp LacY.

Titration of the double-Trp mutant with either Nb by ITC in the absence (**black**) or presence (**gray**) of melibiose yields exothermic titration thermograms (Fig. 2c, i). The heat changes are due specifically to Nb binding to the mutant since consecutive injection of Nb into the assay buffers without protein yields flat thermograms (Fig. 2c, i, **inset**). The accumulated heat change (ΔQ on the right side) as a function of the molar ratio of Nb to LacY fits a one-site independent binding model (Fig. 2d, j), yielding a binding stoichiometry near unity.

Binding of Nb-9036 in the absence of melibiose exhibits a dissociation constant (K_d) of 59.8 ± 5.1 nM (Table 1), which is driven by a favorable enthalpy (ΔH, −49.4 ± 0.3 kJ/mol) with

an entropy penalty ($-T\Delta S$, 8.2 ± 0.5 kJ/mol). The presence of melibiose does not affect binding affinity, but binding is slightly more enthalpic with more entropy compensation (Fig. 2e). With Nb-9065, the K_d is 2- or 5-fold higher than observed with Nb-9036 in the absence or presence of melibiose, respectively, and is also driven by enthalpy at an entropic cost (Fig. 2k).

Nb binding to WT LacY.

Titration of WT LacY with Nb-9036 or 9065 (Fig. 2f-h, l-n) causes a small release of heat (**black**), which is significantly increased by melibiose binding (**gray**). The K_d for Nb-9036 binding is 114.4 ± 6.2 nM, which is decreased by a half to a third in the presence of melibiose (Table 1). The K_d for Nb-9065 binding is 896.5 ± 173.6 nM, which is decreased by melibiose binding to about that of the mutant. Interestingly, binding of both Nbs to the WT in the absence or presence of melibiose is driven by both enthalpy and entropy (Fig. 2h, n), which is different from binding with the mutant, in particular for Nb-9065, where increased entropy constitutes the main driving force in the absence of sugar. Melibiose binding significantly decreases the entropic contribution from 49% to 10% with Nb-9036 and 64% to 20% with Nb-9065 (Table 1).

To illustrate complex formation directly, SDS-PAGE and Blue Native PAGE (BN-PAGE) were used to analyze formation of the protein complexes. On SDS-PAGE, both the WT and the mutant (46.5 kDa) migrate with a M_r of ~35 kDa (lanes 1 and 2). Nb-9036 (~14.9 kDa) and Nb-9065 (~15.1 kDa) migrate with a M_r of around 15 kDa (Fig. 4a). On the BN-PAGE (Fig. 4b), the Nbs migrate as diffuse bands (lanes 1 and 2); the WT and the double-Trp mutant migrate as relatively focused bands (lanes 3 and 6). Both permeases shift to higher M_rs when pre-mixed with either Nb (lanes 4, 5, 7, 8), demonstrating that both proteins form stable complexes with either Nb.

Effect of Nb on galactoside affinity.

α-NPG binding to LacY has been determined by ITC[17, 18]. The WT or the double-Trp mutant binds α-NPG with a K_d of 28.8 ± 2.1 or 5.0 ± 0.5 μM, respectively (Fig. 6 and Table 2), levels similar to those obtained by other methods[3, 17, 18, 48–50], and titration with nitrophenyl-α-D-glucopyranoside yields a small, relatively flat thermogram (Fig. 6). Energetically, α-NPG binding is favored by both enthalpy and entropy with the WT and by enthalpy at an entropic cost with the mutant. As shown previously[17, 18], the stoichiometry of α-NPG binding determined by ITC does not approach unity for unknown reasons, but crystal structures[7, 8] and biochemical studies[49, 50] exhibit only a single galactoside-binding site. While this may alter absolute values of the thermodynamic parameters, the Nb effects on energy changes provide useful information.

When a pre-incubated complex of Nb-9036 with WT or the mutant is titrated with α-NPG (Fig. 6), a K_d of ~0.3 μM with both permease complexes is obtained, an approximate 96- or 19-fold decrease (i.e., increase in affinity), respectively (Table 2). Interestingly, titration of either the Nb-9065:WT or the Nb-9065:mutant complex with α-NPG yields a K_d similar to that of the mutant alone (i.e., a 4-fold decrease with the WT and no detectable change with the mutant). Thermodynamically, α-NPG binding with the complexes, except for the mutant

complexed with Nb-9065, is driven by greater enthalpy ($\Delta\Delta H$ in a range of −29.6 to −38.7 kJ/mol) at a higher entropic cost ($-T\Delta\Delta S$ in a range of 22.4 to 31.3 kJ/mol) (Table 2, Fig. 6d). With α-NPG binding to the mutant complexed with Nb-9065, $\Delta\Delta G$, $\Delta\Delta H$, and $T\Delta\Delta S$ values are very small (Fig. 2h), reflecting the lack of effect of Nb-9065 on binding of α-NPG[15].

Interplay of Nb and IIA^{Glc} binding to LacY.

A previous study[18] shows that IIA^{Glc} does not bind to the double-Trp mutant, but binding to the cytoplasmic face of the WT is endothermic. To determine whether WT LacY can interact simultaneously with IIA^{Glc} and an Nb, the WT pre-equilibrated with Nb-9036 or 9065 in the presence of 10 mM melibiose was titrated with IIA^{Glc}, which exhibits flat exothermic thermograms (Fig. 4) indicating no IIA^{Glc} binding.

Titration of the IIA^{Glc}:WT LacY complex with Nb-9036 in the presence of melibiose shows that IIA^{Glc} has little effect on the Nb binding (Table 3). However, IIA^{Glc} inhibits binding affinity for Nb-9065 by 13-fold, as the result of a large decrease in enthalpy (Fig. 4c). The data clearly suggest that Nb-9036 and Nb-9065 bind to different epitopes in LacY.

Water dynamics in internal cavities of LacY.

To identify the major contributors to the increase in entropy during ligand binding to WT LacY, the dynamics of water molecules and LacY in the two principal inward- and outward-facing states were analyzed by molecular dynamics (MD) simulations (Fig. 5a). The simulations were not designed to measure entropy quantitatively, but rather find a qualitative molecular explanation for the quantitative experiments. In order to simulate the outward-facing state, the crystal structure of the double-Trp mutant with an occluded α-NPG molecule (PDB ID: 4ZYR)[8] was “mutated” back to the WT. The simulation of the outward-facing state resulted in a slightly larger periplasmic cavity than that observed in the crystal structure (Figs. 1b, 5b, Supplemental Fig. S1). It may not represent a completely realistic structural state due to limited temporal sampling. The previous simulation for an inward-facing state[31], which is based on the inward-facing crystal structure of WT apo LacY (PDB ID: 2V8N)[3], was extended to over 200 ns. The simulated inward-facing state exhibits a smaller cytoplasmic cavity as described previously[31].

The water-filled cytoplasmic or periplasmic cavities are divided into a central inner cavity at dimensions of 15 × 15 × 6 Å and an outer region referred to as cytoplasmic or periplasmic gate region, respectively (Fig. 5, **upper panels**). The inner central cavities of both states are composed of the same residues. In the simulated inward- or outward-facing state, the number of water molecules in the central cavity is about 31 ± 3 or 21 ± 7, respectively (blue line; Fig. 5a, b, **middle panel**). The lesser number of water molecules in the simulated outward-facing state is probably due to the presence of α-NPG. These results indicate that the number of water molecules in the common inner cavity remains relatively constant.

To characterize the water dynamics associated with the gate regions, the number of water molecules and residence times during the final 10 ns of each simulation were calculated (Fig. 5, **lower panels**). In the outward-facing state, the hydration dynamics in the

periplasmic gate region is dominated by a large body of water molecules exhibiting shorter residence times, which indicates an efficient exchange between the protein cavity and the surrounding bulk water. In contrast, the water molecules associated with the cytoplasmic gate region in the simulated cytoplasmic-facing state show significantly higher residence times compared to that in the periplasmic gate region, implying a greater number of water molecules with reduced entropy.

The protein motions are analyzed by RMSD calculations for each trajectory with respect to the first simulation frame of the final 10 ns of each simulation. The simulated inward-facing state shows somewhat more pronounced conformational flexibility compared to that in the simulated outward-facing state (Suppl. Fig. S2). Hence, the simulations predict the entropy increase associated with the Nb-induced conformational transition from inward- to outward-facing states to be caused by release of immobilized water rather than an increase in conformational flexibility. In addition, conformational flexibility may be further decreased by binding of the Nb.

Discussion

Release of trapped water molecules from proteins into the bulk solvent causes an increase in entropy because the motion-restricted water molecules on protein surfaces have less freedom (i.e., entropy) than that in the bulk water phase. Therefore, as demonstrated[51], water molecules within the SecY translocon exhibit anomalous diffusion with highly retarded rotational dynamics. For ligand binding, a common interpretation for the increase in entropy is based on the hydrophobic effect at the binding interface (i.e., ordered water molecules are released as hydrophobic groups interact)[26–28]. But water molecules released from a protein may also result from structural rearrangements, such as the closure of hydrophilic cavities, in addition to the release of bound water from a binding interface or other regions. This consideration is especially important for transport proteins like permeases in the major facilitator superfamily[25, 52–55] represented by LacY. These proteins have relatively larger water-filled cavities, and the transport cycles very likely involve formation of occluded intermediates and reciprocal opening and closing of cytoplasmic and periplasmic gate regions (Figs. 1, 5). Previous findings regarding IIA^{Glc} interaction with WT LacY or MelB suggest a correlation between the increase in solvation entropy and the global conformational changes required for IIA^{Glc} binding[18]. Nb binding to LacY provides further support for this interpretation.

The resting state of WT LacY in the absence of substrate is inward-facing conformation, while the resting state of the double-Trp mutant favors the opposite outward-facing conformation[3, 9] (Fig. 6a, b; A), and galactoside binding is believed to induce both permeases to assume an occluded intermediate conformation (Fig. 6a, b; C)[10]. Stopped-flow measurements[15] of galactoside binding suggest that Nb-9036 stabilizes similar outward-facing conformations with either the WT or the double-Trp mutant (Fig. 6a, b; B) and that galactoside binding also induces a similar occluded intermediate with either the WT or the double-Trp mutant complexed with Nb-9036 (Fig. 6a, b; D).

While the binding affinity of Nb-9036 with either permease is similar, the entropy and enthalpy contributing to the binding free energy differs (Table 1, Fig. 6a, b; A→B, C→D). Binding to the outward-facing conformation of WT LacY (from an initial inward-facing state) is driven by both favorable enthalpy and entropy. In contrast, binding to the outward-facing conformation of the mutant (from an outward-facing conformation) is driven by a greater enthalpy with an entropic cost. Furthermore, when the WT is shifted into an occluded intermediate conformation by galactoside binding (state C), Nb-9036 binding is driven by greater enthalpy ($\Delta\Delta H = -18.0$ kJ/mol) at a higher cost of entropy ($-T\Delta\Delta S = 15.3$ kJ/mol), indicating that the galactoside binding promotes binding of Nb-9036. With the double-Trp mutant that is already in an outward-facing conformation (Fig. 6b; A)[13], the effect of galactoside binding on enthalpy and entropy is smaller. In addition, direct measurements of galactoside binding (Table 2) with the inward-facing WT show that formation of the fully liganded occluded state is driven by both favorable enthalpy and entropy. These binding energetics indicate that the increase in entropy correlates with the conformational change in WT LacY that closes the water-filled cytoplasmic gate region to form the occluded intermediate.

To identify the possible origins of the observed entropy increase, MD simulations of inward- and outward-facing conformations were performed. The water dynamics in the narrow, tunnel-like cytoplasmic gate region are significantly retarded (Fig. 5a, lower panel). It is conceivable that these immobilized water molecules will be released during the cytoplasmic closure, and then gain entropy. This process is expected at a time scale of milliseconds, and it is out of reach for the current simulations. The simulated outward-facing state displays a periplasmic gate region that holds a large amount of water molecules with significantly shorter residence times, suggesting little difference between these cavity water and bulk waters. Furthermore, while the Nb-bound structure is not available, RMSD calculations of the last 10-ns simulations suggest that the outward-facing state displays a lesser degree of conformational dynamics compared to that in the inward-facing state. In addition, binding of Nb might reduce this conformational flexibility further. Thus, greater entropic gain from water molecules released from LacY must compensate for the entropy loss due to hydration in the periplasmic gate region and for the loss in protein conformation dynamics. Since the cytoplasmic gate is the major region of the protein undergoing large structural changes that involve dehydration during the inward to outward transition, it is likely that the release of immobilized water from this cytoplasmic gate region is the primary factor contributing to the observed entropy increase associated with Nb binding to WT LacY. It should be noted that a collective release or gain of water molecules in many places of LacY during the structural rearrangement as well as the LacY-Nb interactions may also contribute to the overall entropy increase to a lesser extent. Previously, a high solvation entropy for IIA^{Glc} binding to WT LacY was detected[18]. The current results are consistent with the previous notion that the larger number of bound water molecules released from LacY is primarily the result of closure of the cytoplasmic cavity[18].

Nb-9065 binding to WT or the double-Trp mutant follows a trend similar to that of Nb-9036 binding. Galactoside binding causes insignificant changes in enthalpy and entropy of Nb-9065 binding with the mutant, but increases the affinity of WT for Nb-9065 to a level similar to that of the mutant, at a high cost of entropy ($-T\Delta\Delta S = 14.5$ kJ/mol) (Table 1). The

data further support the conclusion that the favorable entropy observed with the WT likely results from a large conformational change from the resting inward-facing state to the outward-facing state.

When WT LacY or the double-Trp mutant is complexed with Nb-9036, galactoside binding exhibits similar affinities, resulted from a largely increased enthalpy ($\Delta\Delta H = -38.7$ or -29.6 kJ/mol, respectively) at a higher entropic cost ($-T\Delta\Delta S = 27.5$ or 22.4 kJ/mol, respectively) (Fig. 6a, b), indicating positive coupling between the galactoside binding and Nb-9036 binding. Nb-9065 also increases galactoside affinity of WT LacY to a level similar to that of the double-Trp mutant (Table 2), which further supports the previous conclusion that both permeases probably assume similar conformations when Nb-9065 is bound, as is the case for Nb-9036[15] (Fig. 6a, b; B).

The energy contribution to move the state A to D can be further analyzed by comparing the total ΔG value from A-B-D path (Nb bound prior to sugar binding, state A to B to D) and ACD path (sugar bound prior to Nb binding, state A to C to D). With Nb-9065, the $\Delta G_{[ABD]}$ and $\Delta G_{[ACD}]$ values are similar within experimental error for either WT or mutant (Fig. 6c), which conforms to a thermodynamic cycle. With Nb-9036, the $\Delta G_{[ABD]}$ value is significantly greater than $\Delta G_{[ACD]}$ ($\Delta\Delta G_{[ABD]-[ACD]} = -8.5$ or -7.2 kJ/mol for the WT or mutant, respectively, Fig. 6c). Thus, Nb-9036 interrupts the thermodynamic cycle by empowering LacY with a much greater galactoside-binding affinity. Although the precise reason is unknown, Nb-9036 may provide extra contacts to galactoside and/or generate a narrower diffusion pathway for bound sugar.

Taken together, these thermodynamic and molecular dynamics simulation studies suggest that the observed entropy increase coincident with ligand binding to LacY originates mainly from opposition of protein surfaces upon closure of the cytoplasmic cavity and release of immobilized water molecules.

Supplementary Material

Refer to Web version on PubMed Central for supplementary material.

Acknowledgments

Funding Source Statement: This work was supported by the National Science Foundation (grant MCB-1158085 to L.G., Eager grant MCB-1547801 to H.R.K.), the National Institutes of Health (grant R01 GM095538 to L.G. and grant R01 DK51131 to H.R.K.) and a grant from Ruth and Bucky Stein (to H.R.K.). Marie Curie Career Integration Grant (FP7-MC-CIG-618558) and Åke Wibergs Stiftelse (M15-0148) to M.A. MD simulations were supported in part by NSF through TeraGrid (now Xsede) resources provided by the Texas Advanced Computing Center at the University of Texas at Austin. We thank Instruct, part of the European Strategy Forum on Research Infrastructures (ESFRI), and the Hercules Foundation Flanders for their support.

Abbreviations

Nbs	recombinant variable fragments of camelid nanobodies which consist of heavy chain only (devoice with no light chains)
LacY	lactose permease of *Escherichia coli*

MelB	melibiose permease
IIA^{Glc}	a phosphotransferase protein of the glucose-specific phosphoenolpyruvate:carbohydrate phosphotransferase system
α-NPG	nitrophenyl-α-galactoside
DMSO	dimethyl sulfoxide
BN-PAGE	blue native-PAGE
ITC	isothermal titration calorimetry
Δ*H*	enthalpy change
Δ*S*	entropy change
Δ*G*	free energy change
Δ*Q*	accumulated heat change
K_a	association constant
K_d	dissociation constant
MD	simulation, molecular dynamics simulation
RMSD	root mean square deviation.

References

[1]. Kaback HR, Sahin-Toth M, and Weinglass AB (2001) The kamikaze approach to membrane transport, Nat Rev Mol Cell Biol 2, 610–620. [PubMed: 11483994]

[2]. Guan L, and Kaback HR (2006) Lessons from lactose permease, Annu Rev Biophys Biomol Struct 35, 67–91. [PubMed: 16689628]

[3]. Guan L, Mirza O, Verner G, Iwata S, and Kaback HR (2007) Structural determination of wild-type lactose permease, Proc Natl Acad Sci U S A 104, 15294–15298. [PubMed: 17881559]

[4]. Abramson J, Smirnova I, Kasho V, Verner G, Kaback HR, and Iwata S (2003) Structure and mechanism of the lactose permease of *Escherichia coli*, Science 301, 610–615. [PubMed: 12893935]

[5]. Chaptal V, Kwon S, Sawaya MR, Guan L, Kaback HR, and Abramson J (2011) Crystal structure of lactose permease in complex with an affinity inactivator yields unique insight into sugar recognition, Proc Natl Acad Sci U S A 108, 9361–9366. [PubMed: 21593407]

[6]. Mirza O, Guan L, Verner G, Iwata S, and Kaback HR (2006) Structural evidence for induced fit and a mechanism for sugar/H(+) symport in LacY, EMBO J 25, 1177–1183. [PubMed: 16525509]

[7]. Kumar H, Kasho V, Smirnova I, Finer-Moore JS, Kaback HR, and Stroud RM (2014) Structure of sugar-bound LacY, Proc Natl Acad Sci U S A 111, 1784–1788. [PubMed: 24453216]

[8]. Kumar H, Finer-Moore JS, Kaback HR, and Stroud RM (2015) Structure of LacY with an alpha-substituted galactoside: Connecting the binding site to the protonation site, Proc Natl Acad Sci U S A 112, 9004–9009. [PubMed: 26157133]

[9]. Smirnova I, Kasho V, and Kaback HR (2011) Lactose permease and the alternating access mechanism, Biochemistry 50, 9684–9693. [PubMed: 21995338]

[10]. Kaback HR (2015) A chemiosmotic mechanism of symport, Proc Natl Acad Sci U S A 112, 1259–1264. [PubMed: 25568085]

[11]. Zhou Y, Guan L, Freites JA, and Kaback HR (2008) Opening and closing of the periplasmic gate in lactose permease, Proc Natl Acad Sci U S A 105, 3774–3778. [PubMed: 18319336]

[12]. Jiang X, Nie Y, and Kaback HR (2011) Site-directed alkylation studies with LacY provide evidence for the alternating access model of transport, Biochemistry 50, 1634–1640. [PubMed: 21254783]

[13]. Smirnova I, Kasho V, Sugihara J, and Kaback HR (2013) Trp replacements for tightly interacting Gly-Gly pairs in LacY stabilize an outward-facing conformation, Proc Natl Acad Sci U S A 110, 8876–8881. [PubMed: 23671103]

[14]. Kaback HR, Smirnova I, Kasho V, Nie Y, and Zhou Y (2011) The alternating access transport mechanism in LacY, J Membr Biol 239, 85–93. [PubMed: 21161516]

[15]. Smirnova I, Kasho V, Jiang X, Pardon E, Steyaert J, and Kaback HR (2014) Outward-facing conformers of LacY stabilized by nanobodies, Proc Natl Acad Sci U S A 111, 18548–18553. [PubMed: 25512549]

[16]. Smirnova I, Kasho V, Jiang X, Pardon E, Steyaert J, and Kaback HR (2015) Transient conformers of LacY are trapped by nanobodies, Proc Natl Acad Sci U S A 112, 13839–13844. [PubMed: 26512108]

[17]. Nie Y, Smirnova I, Kasho V, and Kaback HR (2006) Energetics of ligand-induced conformational flexibility in the lactose permease of *Escherichia coli*, J Biol Chem 281, 35779–35784. [PubMed: 17003033]

[18]. Hariharan P, Balasubramaniam D, Peterkofsky A, Kaback HR, and Guan L (2015) Thermodynamic mechanism for inhibition of lactose permease by the phosphotransferase protein IIA(Glc), Proc Natl Acad Sci U S A 112, 2407–2412. [PubMed: 25675534]

[19]. Hariharan P, and Guan L (2014) Insights into the inhibitory mechanisms of the regulatory protein IIA(Glc) on melibiose permease activity, J Biol Chem 289, 33012–33019. [PubMed: 25296751]

[20]. Chao Y, and Fu D (2004) Thermodynamic studies of the mechanism of metal binding to the *Escherichia coli zinc* transporter YiiP, J Biol Chem 279, 17173–17180. [PubMed: 14960568]

[21]. Boudker O, and Oh S (2015) Isothermal titration calorimetry of ion-coupled membrane transporters, Methods 76, 171–182. [PubMed: 25676707]

[22]. Pourcher T, Leclercq S, Brandolin G, and Leblanc G (1995) Melibiose permease of *Escherichia coli*: large scale purification and evidence that H(+), Na(+), and Li(+) sugar symport is catalyzed by a single polypeptide, Biochemistry 34, 4412–4420. [PubMed: 7703254]

[23]. Maehrel C, Cordat E, Mus-Veteau I, and Leblanc G (1998) Structural studies of the melibiose permease of *Escherichia coli* by fluorescence resonance energy transfer. I. Evidence for ion-induced conformational change, J Biol Chem 273, 33192–33197. [PubMed: 9837887]

[24]. Guan L, Nurva S, and Ankeshwarapu SP (2011) Mechanism of melibiose/cation symport of the melibiose permease of *Salmonella typhimurium*, J Biol Chem 286, 6367–6374. [PubMed: 21148559]

[25]. Ethayathulla AS, Yousef MS, Amin A, Leblanc G, Kaback HR, and Guan L (2014) Structure-based mechanism for Na(+)/melibiose symport by MelB, Nat Commun 5, 3009. [PubMed: 24389923]

[26]. Dam TK, Torres M, Brewer CF, and Casadevall A (2008) Isothermal titration calorimetry reveals differential binding thermodynamics of variable region-identical antibodies differing in constant region for a univalent ligand, J Biol Chem 283, 31366–31370. [PubMed: 18806257]

[27]. Jelesarov I, and Bosshard HR (1994) Thermodynamics of ferredoxin binding to ferredoxin:NADP(+) reductase and the role of water at the complex interface, Biochemistry 33, 13321–13328. [PubMed: 7947740]

[28]. Olsson TS, Williams MA, Pitt WR, and Ladbury JE (2008) The thermodynamics of protein-ligand interaction and solvation: insights for ligand design, J Mol Biol 384, 1002–1017. [PubMed: 18930735]

[29]. Pardon E, Laeremans T, Triest S, Rasmussen SG, Wohlkonig A, Ruf A, Muyldermans S, Hol WG, Kobilka BK, and Steyaert J (2014) A general protocol for the generation of Nanobodies for structural biology, Nat Protoc 9, 674–693. [PubMed: 24577359]

[30]. Schagger H, and von Jagow G (1991) Blue native electrophoresis for isolation of membrane protein complexes in enzymatically active form, Anal Biochem 199, 223–231. [PubMed: 1812789]

[31]. Andersson M, Bondar AN, Freites JA, Tobias DJ, Kaback HR, and White SH (2012) Proton-coupled dynamics in lactose permease, Structure 20, 1893–1904. [PubMed: 23000385]

[32]. Sali A, and Blundell TL (1993) Comparative protein modelling by satisfaction of spatial restraints, J Mol Biol 234, 779–815. [PubMed: 8254673]

[33]. Yesselman JD, Price DJ, Knight JL, and Brooks CL 3rd. (2012) MATCH: an atom-typing toolset for molecular mechanics force fields, J Comput Chem 33, 189–202. [PubMed: 22042689]

[34]. Jiang X, Villafuerte MK, Andersson M, White SH, and Kaback HR (2014) Galactoside-binding site in LacY, Biochemistry 53, 1536–1543. [PubMed: 24520888]

[35]. Jo S, Kim T, and Im W (2007) Automated builder and database of protein/membrane complexes for molecular dynamics simulations, PLoS One 2, e880. [PubMed: 17849009]

[36]. Phillips JC, Braun R, Wang W, Gumbart J, Tajkhorshid E, Villa E, Chipot C, Skeel RD, Kale L, and Schulten K (2005) Scalable molecular dynamics with NAMD, J Comput Chem 26, 1781–1802. [PubMed: 16222654]

[37]. Mackerell AD Jr., Feig M, and Brooks CL 3rd. (2004) Extending the treatment of backbone energetics in protein force fields: limitations of gas-phase quantum mechanics in reproducing protein conformational distributions in molecular dynamics simulations, J Comput Chem 25, 1400–1415. [PubMed: 15185334]

[38]. Klauda JB, Venable RM, Freites JA, O'Connor JW, Tobias DJ, Mondragon-Ramirez C, Vorobyov I, MacKerell AD Jr., and Pastor RW (2010) Update of the CHARMM all-atom additive force field for lipids: validation on six lipid types, J Phys Chem B 114, 7830–7843. [PubMed: 20496934]

[39]. Jorgensen W, Chandrasekhar J, Madura J, Impey R, and Klein M (1983) Comparison of simple potential functions for simulating liquid water, J. Chem Phys 79, 926–935.

[40]. Grubmüller H, Heller H, Windemuth A, and Schulten K (1991) Generalized Verlet Algorithm for Efficient Molecular Dynamics Simulations with Long-range Interactions, Molecular Simulation 6, 121–142.

[41]. Darden T, York D, and Pedersen L (1993) Particle mesh Ewald: An N·log(N) method for Ewald sums in large systems, J Chem Phys 98, 10089–10092.

[42]. Essmann U, Perera L, Berkowitz M, Darden T, Lee H, and Pedersen L (1995) A smooth particle mesh Ewald method, J Chem Phys 103, 8577–8593.

[43]. Ryckaert J-P, Ciccotti G, and Berendsen H (1977) Numerical integration of the cartesian equations of motion of a system with constraints: molecular dynamics of n-alkanes, J Comput Phys 23, 327–341.

[44]. Miyamoto S, and Kollman P (1992) Settle: An analytical version of the SHAKE and RATTLE algorithm for rigid water models, J. Comput. Chem 13, 952–962.

[45]. Feller S, Zhang Y, Pastor R, and Brooks B (1995) Constant pressure molecular dynamics simulation: The Langevin piston method, J Chem Phys 103, 4613–4621.

[46]. Martyna G, Tobias D, and Klein M (1994) Constant pressure molecular dynamics algorithms, J Chem Phys 101, 4177–4189.

[47]. Humphrey W, Dalke A, and Schulten K (1996) VMD: Visual molecular dynamics, J Mol Graphics 14, 33–38.

[48]. Smirnova IN, Kasho V, and Kaback HR (2008) Protonation and sugar binding to LacY, Proc Natl Acad Sci U S A 105, 8896–8901. [PubMed: 18567672]

[49]. Sahin-Toth M, Lawrence MC, Nishio T, and Kaback HR (2001) The C-4 hydroxyl group of galactopyranosides is the major determinant for ligand recognition by the lactose permease of *Escherichia coli*, Biochemistry 40, 13015–13019. [PubMed: 11669639]

[50]. Guan L, and Kaback HR (2004) Binding affinity of lactose permease is not altered by the H+ electrochemical gradient, Proc Natl Acad Sci U S A 101, 12148–12152. [PubMed: 15304639]

[51]. Capponi S, Heyden M, Bondar AN, Tobias DJ, and White SH (2015) Anomalous behavior of water inside the SecY translocon, Proc Natl Acad Sci U S A 112, 9016–9021. [PubMed: 26139523]

[52]. Deng D, Xu C, Sun P, Wu J, Yan C, Hu M, and Yan N (2014) Crystal structure of the human glucose transporter GLUT1, Nature 510, 121–125. [PubMed: 24847886]

[53]. Quistgaard EM, Low C, Moberg P, Tresaugues L, and Nordlund P (2013) Structural basis for substrate transport in the GLUT-homology family of monosaccharide transporters, Nat Struct Mol Biol 20, 766–768. [PubMed: 23624861]

[54]. Nomura N, Verdon G, Kang HJ, Shimamura T, Nomura Y, Sonoda Y, Hussien SA, Qureshi AA, Coincon M, Sato Y, Abe H, Nakada-Nakura Y, Hino T, Arakawa T, Kusano-Arai O, Iwanari H, Murata T, Kobayashi T, Hamakubo T, Kasahara M, Iwata S, and Drew D (2015) Structure and mechanism of the mammalian fructose transporter GLUT5, Nature 526, 397–401. [PubMed: 26416735]

[55]. Pedersen BP, Kumar H, Waight AB, Risenmay AJ, Roe-Zurz Z, Chau BH, Schlessinger A, Bonomi M, Harries W, Sali A, Johri AK, and Stroud RM (2013) Crystal structure of a eukaryotic phosphate transporter, Nature 496, 533–536. [PubMed: 23542591]

[56]. Smirnova I, Kasho V, Sugihara J, and Kaback HR (2011) Opening the periplasmic cavity in lactose permease is the limiting step for sugar binding, Proc Natl Acad Sci U S A 108, 15147–15151. [PubMed: 21896727]

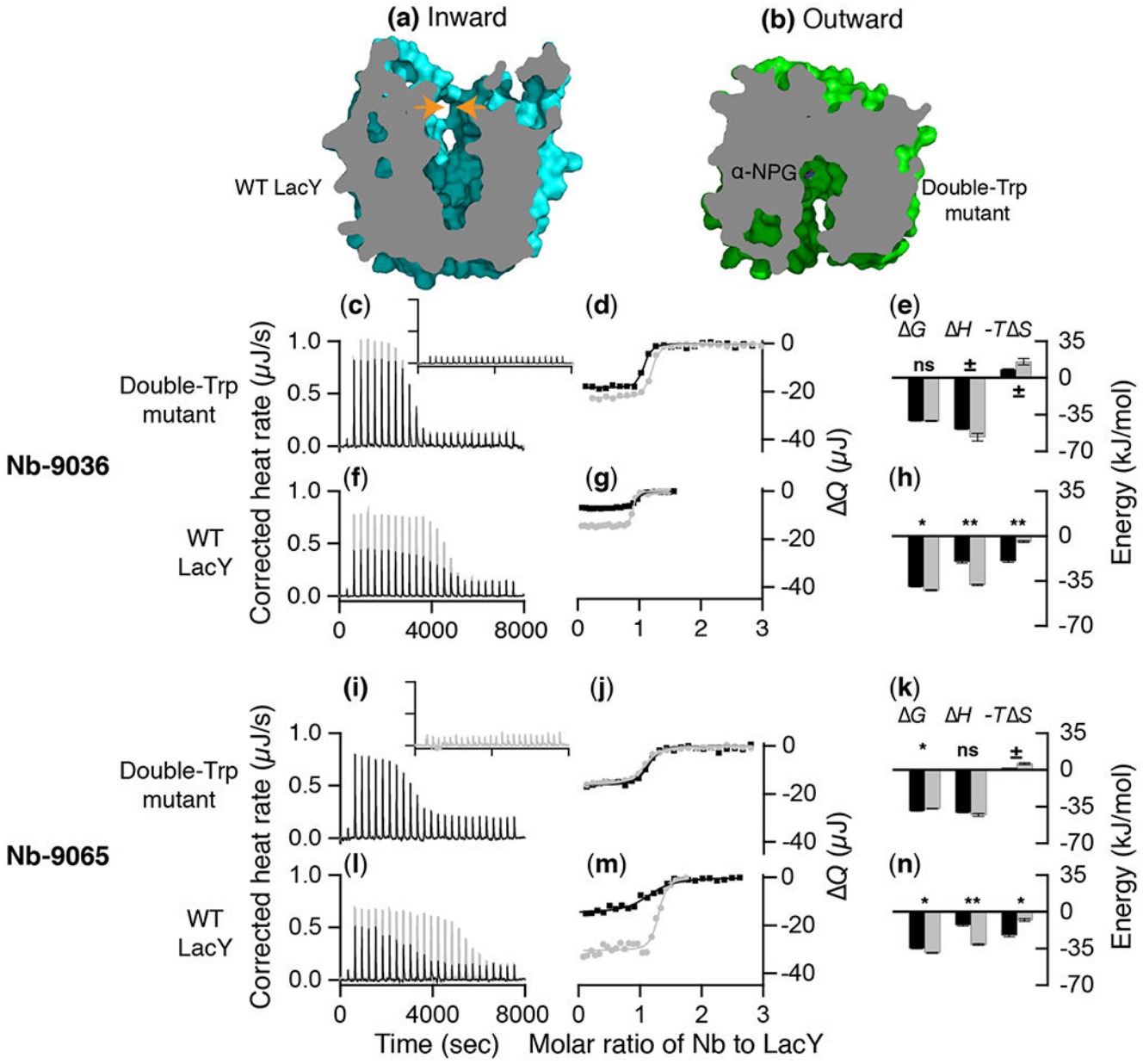

Fig. 1. Nb binding to LacY by ITC.

(a) Cross-section of inward-facing conformation from the X-ray crystal structure of WT apo LacY (pdb, 2V8N)[3] or **(b)** a narrowly outward-facing conformation of G46W/G262W LacY with an occluded α-NPG molecule (pdb, 4ZYR)[8]. The two small orange arrows facing each other in (a) point to the area that closes to form the occluded or outward-facing conformation. **(c-n)** Nb binding. Titration of G46W/G262W LacY (22 or 25 μM) or WT LacY (40 μM) with Nb-9036 (188 μM) or Nb-9065 (200 μM) in the absence (black) or presence (gray) of melibiose at a saturating concentration of 10 mM was performed with a Nano ITC instrument. (**c, f, i, l**) Thermograms were recorded at 25 °C. Inset in **c**, thermogram from the injection of Nb into buffer without protein. (**d, g, j, m**) Accumulated heat change (Δ*Q*, on the right side) plotted against the Nb:LacY molar ratio. The data were

fitted to a one-site independent binding model, and the results were presented in Table 1. (**e, h, k, n**) Comparison of Nb binding energy in the absence (black) and presence (gray) of galactoside. The histograms were generated from data in Table 1. Unpaired *t*-test was applied for the statastic anlaysis. $P > 0.1$, the differenc is considered to be not statistically significant (ns); $0.1 < P > 0.05$, not quite statistically significant ($^{\pm}$); $0.05 < P > 0.01$, statistically significant (*); $0.01 < P > 0.001$, very statistically significant (**).

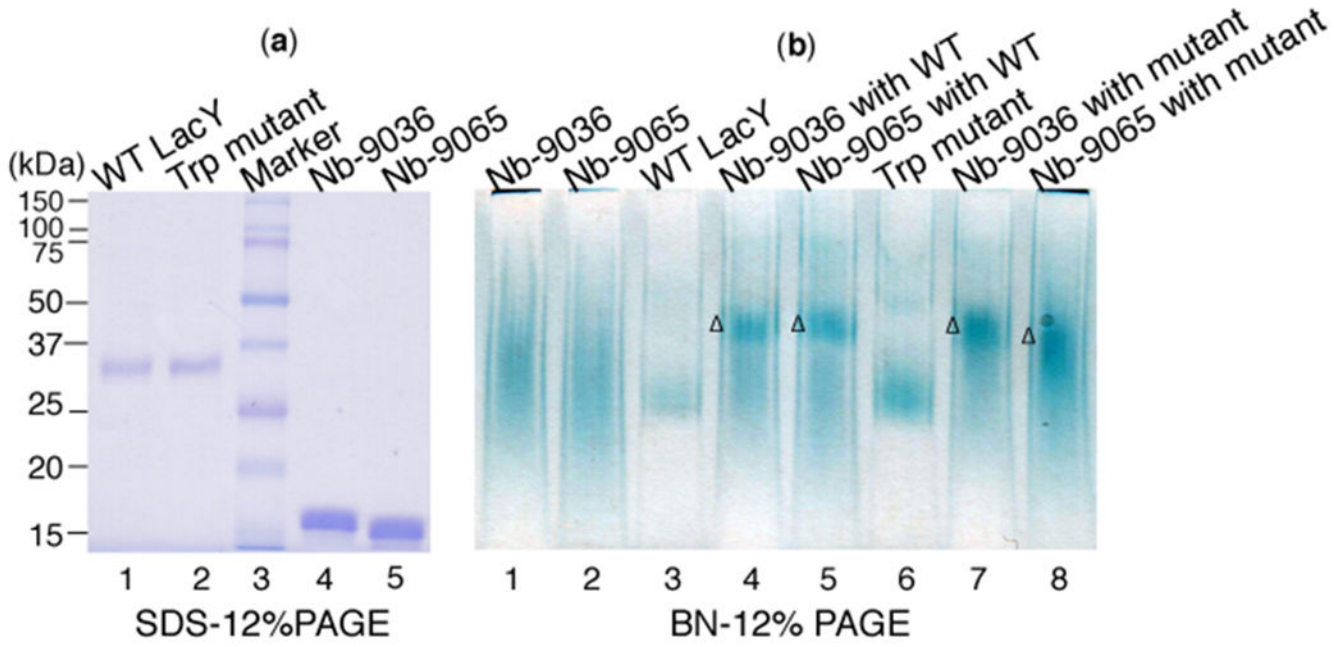

Fig. 2. Nb:LacY complex formation.

(**a**) SDS-12%PAGE. WT LacY or the double-Trp mutant (ca. 1 μg) were loaded in lanes 1 or 2, respectively, without heating. Given Nbs (3 μg) were loaded in lanes 4 or 5 after heating at 95 °C for 15 min in the presence of 5 mM DTT. Molecular weight markers are given in lane 3. (**b**) Blue native-12%PAGE. Nbs (8 μg), WT LacY (4 μg) or the double-Trp mutant (4 μg) were loaded in the indicated lanes. WT LacY or the double-Trp mutant were mixed with a given Nb at a ratio of 1:2 prior to the analysis. Δ, the position of the Nb:LacY complexes.

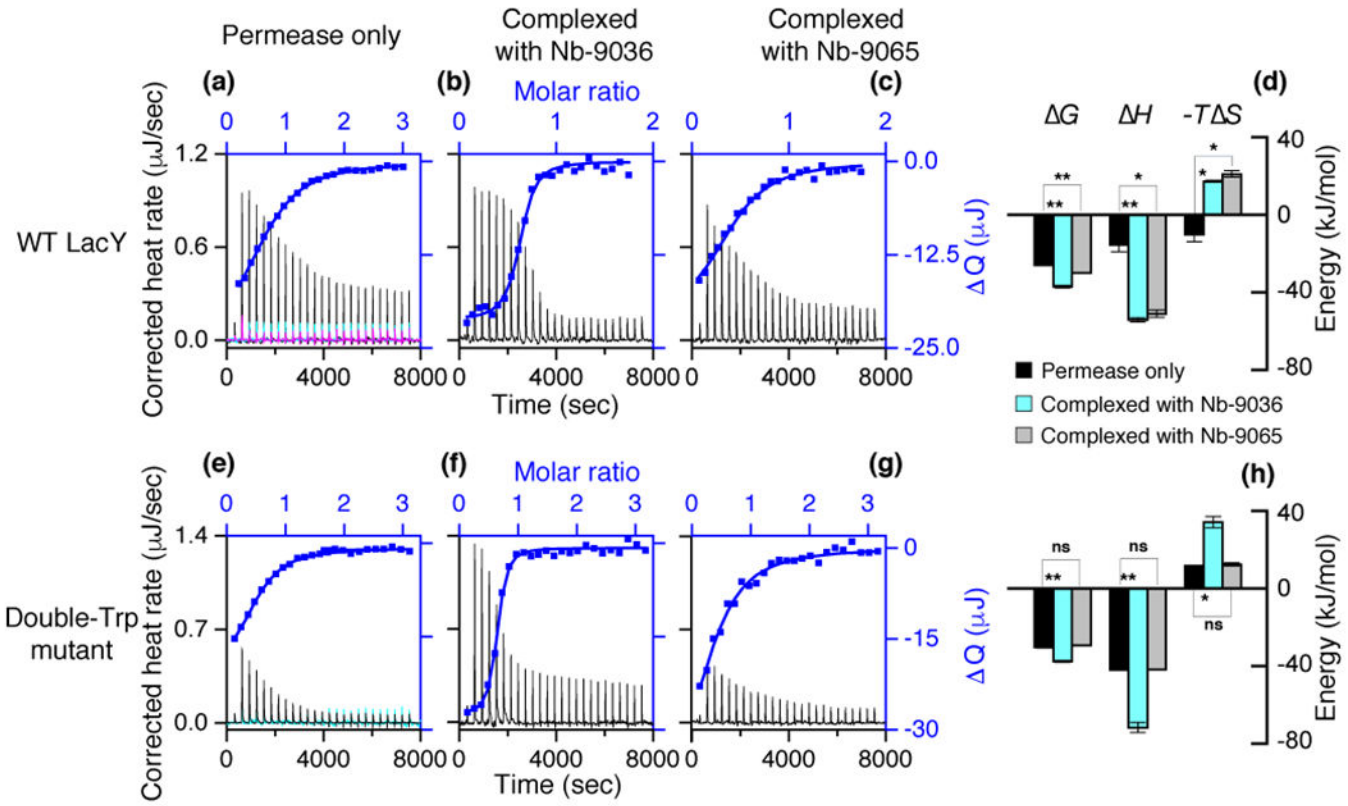

Fig. 3. α-NPG binding in the absence or presence of a bound Nb.

α-NPG at 1 mM or 0.2 mM was injected into the sample cell containing WT LacY (100 μM) or G46W/G262W mutant (28 μM), respectively (**a, e**). WT LacY or the mutant pre-incubated with Nb-9036 (**b, f**) or Nb-9065 (**c, g**) at a ratio of 1:1.75 or 2.5, respectively, was titrated with α-NPG (0.2 mM). DMSO (0.5%) was present in both titrand and titrant for α-NPG solubility. Thermogram (**a-c, e-g**) was recorded at 25 °C. Injection of α-NPG into buffer at a concentration used for the titration into the protein samples is shown in cyan (**a, e**), and injection of 1 mM nitrophenyl-α-glucoside into the WT LacY is shown in magenta (**a**). Δ*Q* (on the right side) vs α-NPG:LacY molar ratio (on the top) were fitted to a one-site independent binding model (blue curves), and the results were presented in Table 2 and panels d and f. (**d, h**) Comparison of α-NPG binding energy in the absence (black) and presence of Nb-9036 (cyan) or Nb-9065 (gray). Unpaired *t*-test was applied for the statastic anlaysis as deacribed in the legand to figure 1.

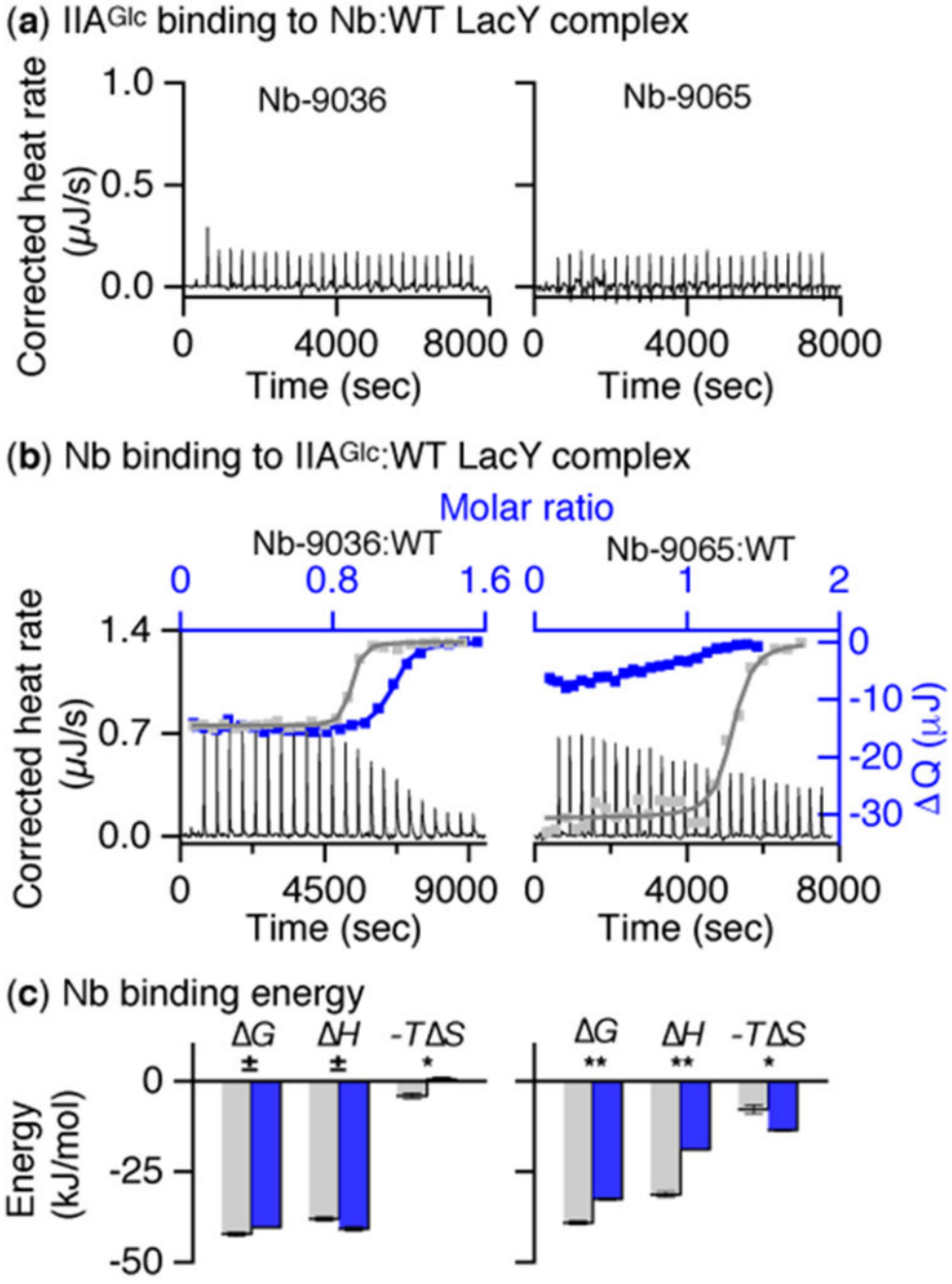

Fig. 4. Interplay of Nb and IIA^{Glc} binding to LacY at 25 °C.

(**a**) IIA^{Glc} titration thermogram. Nb-9036 or Nb-9065 (66 μM) was pre-mixed with LacY (40 μM) in the presence of 10 mM melibiose, and the complex was titrated with IIA^{Glc} (455 μM). (**b**) Nb binding to LacY:IIA^{Glc} complex. LacY (40 μM) pre-incubated with IIA^{Glc} at a ratio of 1:2 was titrated with Nb-9036 (left panel) or Nb-9065 (right panel) at 170 μM in the presence of 10 mM melibiose. ΔQ (right axis) were plotted against the Nb/LacY molar ratio (top axis) and fitted to a one-site independent binding model (blue color). The fitting data from Nb binding to LacY without IIA^{Glc} (gray) were from Figure 1. (**c**) Histogram.

Comparison of Nb binding energy in the absence (gray) and presence (blue) of IIA^{Glc}. Numerical values are presented in Table 3. Unpaired *t*-test was applied for the statastic anlaysis as deacribed in the legand to figure 1.

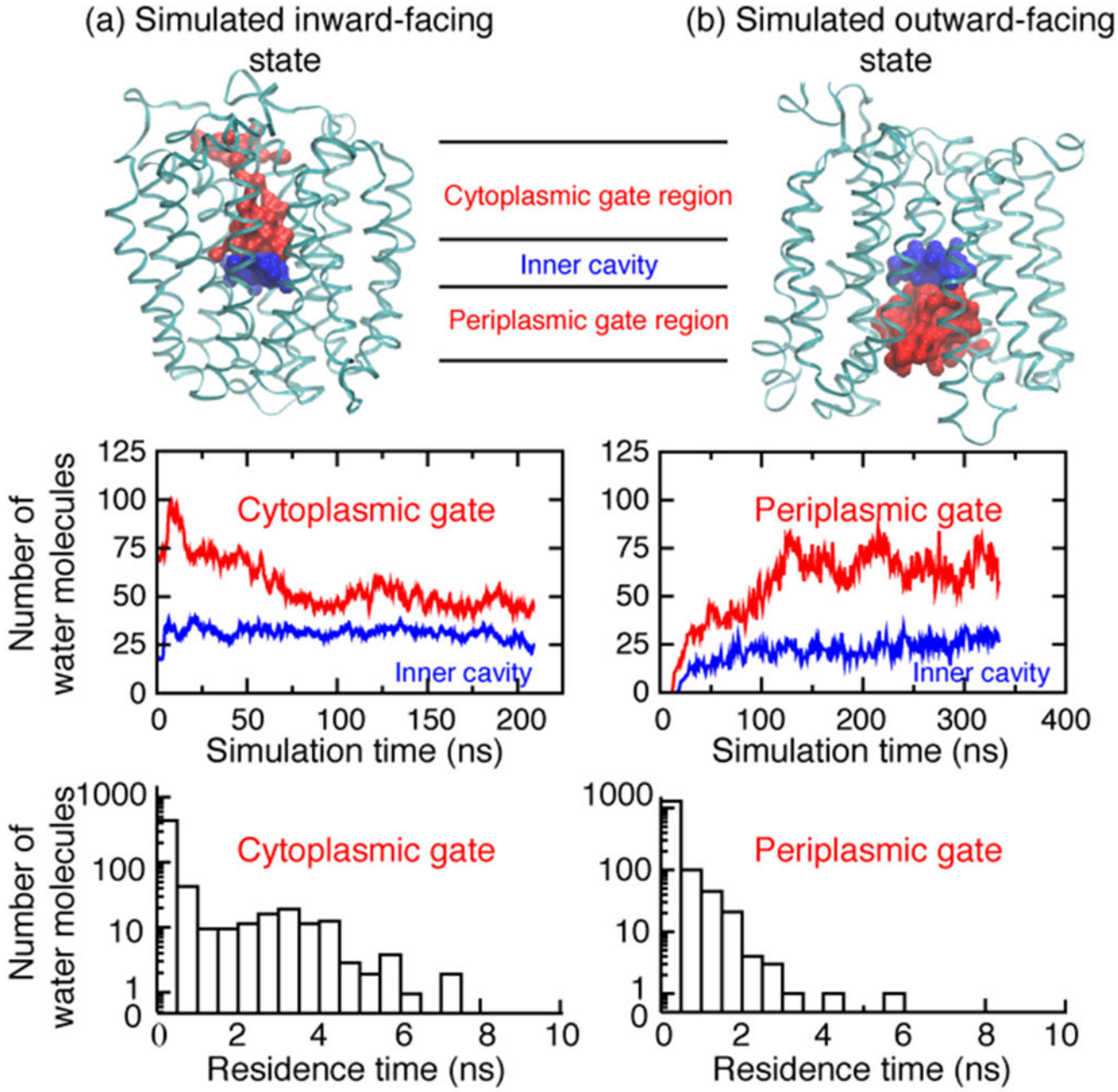

Fig. 5. Water dynamics in LacY internal cavities.

(a) Inward-facing conformation of WT apo LacY. **(b)** Outward-facing conformation of WT LacY with bound α-NPG. **Upper panels**, backbone structure of simulated inward-facing conformation based on crystal structure of WT (pdb, 2N8V) and backbone structure of simulated outward-facing conformation with an occluded α-NPG molecule (derived from pdb, 4ZYR). Water molecules extracted at the end of each simulation are colored in blue (inner cavity) and red (cytoplasmic or periplasmic gate regions). **Middle panels**, number of water molecules in the inner cavities (blue) or the gate regions (red) plotted versus time. **Lower panels**, residence time of water molecules associated with cytoplasmic (left) or

periplasmic gate (right) regions, respectively, presented in histogram with a log plot on the *y* axis.

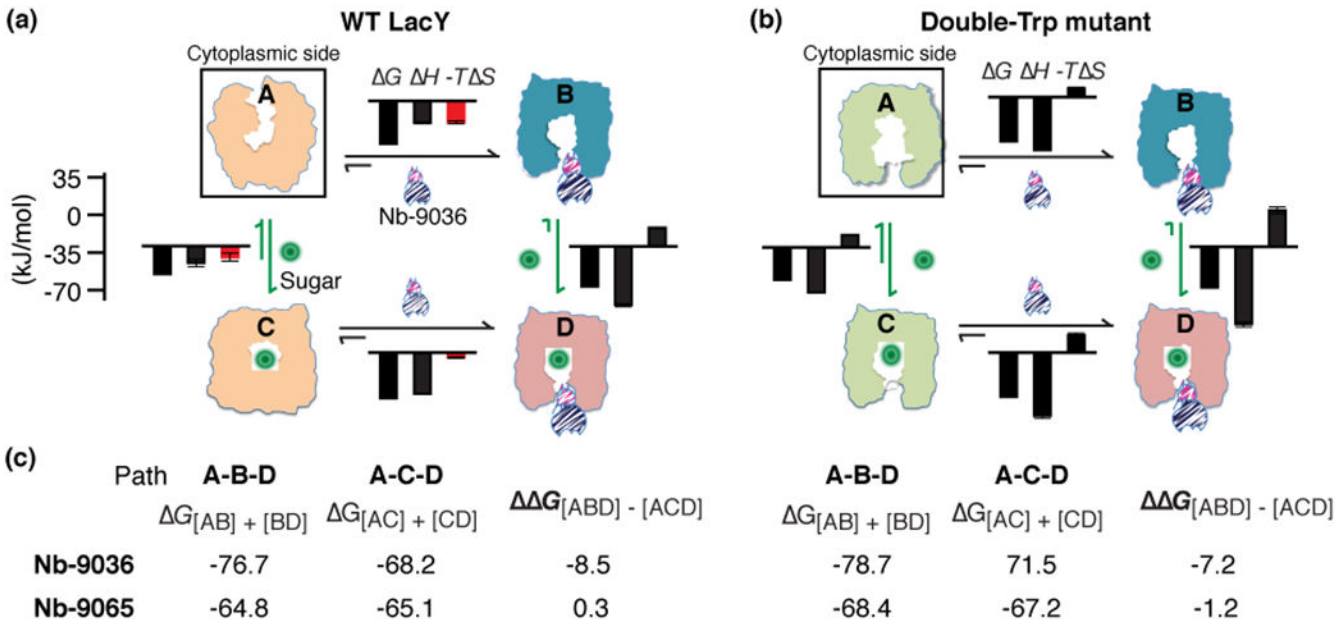

(c)

Path	A-B-D	A-C-D		A-B-D	A-C-D	
	$\Delta G_{[AB]+[BD]}$	$\Delta G_{[AC]+[CD]}$	$\Delta\Delta G_{[ABD]-[ACD]}$	$\Delta G_{[AB]+[BD]}$	$\Delta G_{[AC]+[CD]}$	$\Delta\Delta G_{[ABD]-[ACD]}$
Nb-9036	-76.7	-68.2	-8.5	-78.7	71.5	-7.2
Nb-9065	-64.8	-65.1	0.3	-68.4	-67.2	-1.2

Fig. 6. Thermodynamic cycle of Nbs and galactoside binding to WT or double-Trp LacY.

(a) WT LacY. (**b**) Double-Trp mutant. State A in (a), cartoon of simulated model of WT LacY based on the crystal structure (2V8N) represents an inward-facing, lowest free energy state[3]. State A in *b*, cartoon of simulated double-Trp mutant model of outward-facing state[13, 56]. States B in *a* and *b*, proposed Nb-9036-bound outward-facing conformation[15]. State C in *a* and *b*, cartoons based on crystal structures of double-Trp mutant with occluded galactoside (4OAA, or 4ZYR)[7, 8]. State D in *a* and *b*, occluded intermediate where k_{off} of galactoside is markedly inhibited[15]. Histograms are from Tables 1 and 2, and ΔG, ΔH -$T\Delta S$ are labeled with a scale at the right side. (**c**) Thermodynamic cycle analysis. Conformational change from A to B to D is expressed as the A-B-D path, and from A to C to D is expressed as the A-C-D path. The free energy difference between the two paths is expressed by $\Delta\Delta G_{[ABD]-[ACD]}$. The data for both Nb-9036 and 9065 are from tables 1 and 2.

Table 1.

Nb binding with ITC at 25 °C[a]

Titrant (Syringe)	Titrand (Cell)	Mel (mM)	K_d (mM)	ΔG [$\Delta\Delta G$][b]	ΔH [$\Delta\Delta H$]	$-T\Delta S$ [$-T\Delta\Delta S$]	N
				(kJ/mol)			
Nb-9036	Double-Trp mutant	0	59.8 (5.1[c])	−41.2 (0.2)	−49.4 (0.3)	8.2 (0.5)	1.0 (0.1)
		10	61.2 (8.4)	−41.2 (0.3)	−58.1 (2.6)	16.5 (2.1)	1.0 (0.1)
				[−0.0[ns]]	[−8.7[±]]	[8.3[±]]	
	WT LacY	0	114.4 (6.2)	−39.6 (0.2)	−20.1 (1.0)	−19.5 (1.1)	0.9 (0.1)
		10	39.3 (8.2)	−42.3 (0.5)	−38.1 (0.6)	−4.2 (0.7)	1.0 (0.1)
				[−2.7[*]]	[−18.0[**]]	[15.3[**]]	
Nb-9065	Double-Trp mutant	0	150.4 (15.4)	−39.0 (0.3)	−40.7 (0.2)	1.8 (0.0)	1.1 (0.0)
		10	340.7 (45.4)	−36.9 (0.3)	−42.9 (1.3)	5.9 (1.0)	1.0 (0.0)
				[2.1[*]]	[−2.2[ns]]	[4.1[±]]	
	WT LacY	0	896.5 (173.6)	−34.8 (0.5)	−12.6 (1.2)	−22.3 (1.5)	1.0 (0.1)
		10	138.6 (23.1)	−39.2 (0.5)	−31.4 (0.8)	−7.9 (1.3)	1.2 (0.1)
				[−4.4[*]]	[−18.9[**]]	[14.5[*]]	

[a] Data are from Fig. 1.

[b] Difference in the absence and presence of melibiose;

[c] s.e.m., number of tests = 2-5; N, stoichiometry;

[ns] not statistically significant;

[±] not quite statistically significant;

[*] statistically significant;

[**] very statistically significant.

Table 2.

Effect of Nb on WT LacY affinity for α-NPG[a]

Titrant (Syringe)	Titrand (Sample Cell)	K_d (μM)	ΔG [$\Delta\Delta G$][b]	ΔH [$\Delta\Delta H$]	$-T\Delta S$ [$-T\Delta\Delta S$]	N
			(kJ/mol)			
α-NPG	WT LacY	28.8 (2.1[c])	−25.9 (0.2)	−15.6 (3.4)	−10.3 (3.6)	0.6 (0.1)
	WT:Nb-9036	0.3 (0.1)	−37.1 (0.6)	−54.3 (1.1)	17.2 (0.5)	0.5 (0.1)
			[−11.2 **]	[−38.7 **]	[27.5 *]	
	WT:Nb-9065	5.7 (0.1)	−30.0 (0.1)	−51.0 (1.8)	21.0 (1.7)	0.5 (0.0)
			[−4.1 **]	[−35.4 *]	[31.3 *]	
	Double-Trp mutant	5.0 (0.5)	−30.3 (0.3)	−42.1 (0.0)	11.8 (0.3)	0.5 (0.0)
	Mutant:Nb-9036	0.3 (0.0)	−37.5 (0.4)	−71.7 (2.5)	34.2 (2.9)	0.6 (0.0)
			[−7.2 **]	[−29.6 **]	[22.4 *]	
	Mutant:Nb-9065	7.1 (0.6)	−29.4 (0.2)	−41.8 (1.05)	12.43 (0.9)	0.4 (0.0)
			[0.9 ns]	[0.3 ns]	[0.6 ns]	

[a] Data are from Fig. 3;

[b] Difference in the absence and presence of Nb;

[c] s.e.m., number of tests = 2. N, stoichiometry;

ns not statistically significant;

* statistically significant;

** very statistically significant.

Table 3.

Interplay of IIA^{Glc} and Nb with LacY:melibiose binary complex[a]

Titrant (Syringe)	Titrand (Sample Cell)	K_d (nM)	$\Delta G[\Delta\Delta G]^b$	ΔH [$\Delta\Delta H$]	$-T\Delta S$ [$-T\Delta\Delta S$]	N
			(kJ/mol)			
IIA^{Glc}	WT LacY:Nb-9036	ND	ND	ND	ND	
IIA^{Glc}	WT LacY:Nb-9065	ND	ND	ND	ND	
Nb-9036	WT LacY	39.3 (8.2)	−42.3 (0.5)	−38.1 (0.6)	−4.2 (0.7)	1.0 (0.1)
	WT LacY: IIA^{Glc}	80.5 (1.7)	−40.5 (0.1)	−40.9 (0.5)	0.4 (0.6)	1.0 (0.1)
			[1.8 ±]	[−2.8 ±]	[3.8 *]	
Nb-9065	WT LacY	138.6 (23.1)	−39.2 (0.5)	−31.4 (0.8)	−7.9 (1.3)	1.2 (0.1)
	WT LacY: IIA^{Glc}	1,915.2 (255.2)	−32.7 (0.3)	−19.0 (0.2)	−13.7 (0.2)	0.9 (0.0)
			[6.5 **]	[12.3 **]	[−5.9 *]	

[a] ITC were measured at 25 °C in the presence of 10 mM melibiose and data were presented in Fig. 4;

[b] Difference in the absence and presence of IIA^{Glc};

[c] s.e.m., number of tests = 2-3. N, stoichiometry;

± not quite statistically significant;

* statistically significant;

** very statistically significant.